



# A Generic Multivariate Framework for the Integration of Microbiome Longitudinal Studies With Other Data Types

Antoine Bodein<sup>1†</sup>, Olivier Chapleur<sup>2†</sup>, Arnaud Droit<sup>1</sup> and Kim-Anh Lê Cao<sup>3\*</sup>

<sup>1</sup> Molecular Medicine Department, CHU de Québec Research Center, Université Laval, Québec, QC, Canada,

<sup>2</sup> Hydrosystems and Biopresses Research Unit, Irstea, Antony, France, <sup>3</sup> Melbourne Integrative Genomics, School of Mathematics and Statistics, University of Melbourne, Melbourne, VIC, Australia

## OPEN ACCESS

### Edited by:

Himel Mallick,  
Merck, United States

### Reviewed by:

Gholamali Ali Rahnavard,  
Broad Institute,  
United States  
Lingling An,  
University of Arizona,  
United States

### \*Correspondence:

Kim-Anh Lê Cao  
kimanh.lecao@unimelb.edu.au

<sup>†</sup>These authors have contributed  
equally to this work

### Specialty section:

This article was submitted to  
Statistical Genetics and Methodology,  
a section of the journal  
Frontiers in Genetics

**Received:** 04 April 2019

**Accepted:** 10 September 2019

**Published:** 07 November 2019

### Citation:

Bodein A, Chapleur O, Droit A  
and Lê Cao K-A (2019) A Generic  
Multivariate Framework for the  
Integration of Microbiome  
Longitudinal Studies With  
Other Data Types.  
*Front. Genet.* 10:963.  
doi: 10.3389/fgene.2019.00963

Simultaneous profiling of biospecimens using different technological platforms enables the study of many data types, encompassing microbial communities, omics, and meta-omics as well as clinical or chemistry variables. Reduction in costs now enables longitudinal or time course studies on the same biological material or system. The overall aim of such studies is to investigate relationships between these longitudinal measures in a holistic manner to further decipher the link between molecular mechanisms and microbial community structures, or host-microbiota interactions. However, analytical frameworks enabling an integrated analysis between microbial communities and other types of biological, clinical, or phenotypic data are still in their infancy. The challenges include few time points that may be unevenly spaced and unmatched between different data types, a small number of unique individual biospecimens, and high individual variability. Those challenges are further exacerbated by the inherent characteristics of microbial communities-derived data (e.g., sparse, compositional). We propose a generic data-driven framework to integrate different types of longitudinal data measured on the same biological specimens with microbial community data and select key temporal features with strong associations within the same sample group. The framework ranges from filtering and modeling to integration using smoothing splines and multivariate dimension reduction methods to address some of the analytical challenges of microbiome-derived data. We illustrate our framework on different types of multi-omics case studies in bioreactor experiments as well as human studies.

**Keywords:** time course, data integration, splines, feature selection, dimension reduction, multi-omics

## INTRODUCTION

Microbial communities are highly dynamic biological systems that cannot be fully investigated in snapshot studies. The decreasing cost of DNA sequencing has enabled longitudinal and time-course studies to record the temporal variation of microbial communities (Knight et al., 2012; Faust et al., 2015). These studies can inform us about the stability and dynamics of microbial communities in response to perturbations or different conditions of the host or their habitat. They can also capture the dynamics of microbial interactions (Bucci et al., 2016; Ridenhour et al., 2017) or associated

changes of microbial features, such as taxonomies or genes, to a phenotypic group (Metwally et al., 2018).

However, besides the inherent characteristics of microbiome data, including sparsity, compositionality (Aitchison, 1982; Gloor et al., 2017), its multivariate nature, and high variability (Lê Cao et al., 2016a), longitudinal studies suffer from irregular sampling and subject drop-outs. Thus, appropriate modeling of the microbial profiles is required—for example, by using spline modeling. Methods including loess (Shields-Cutler et al., 2018), smoothing spline ANOVA (Paulson et al., 2017), negative binomial smoothing splines (Metwally et al., 2018), or Gaussian cubic splines (Luo et al., 2017) were proposed to model dynamics of microbial profiles across groups of samples or subjects. The aim of these approaches is to make statistical inferences about global changes of differential abundance across multiple phenotypes of interest, rather than at specific time points. These proposed methods are univariate and, as such, cannot infer ecological interactions (Morris et al., 2016). Other types of methods aim to cluster microbial profiles to posit hypotheses about symbiotic relationships, interaction, or competition. For example, Baksi et al. (2018) used a Jensen–Shannon divergence metric to visually compare metagenomic time series.

Multivariate ordination methods can exploit the interaction between microorganisms but need to be used with sparsity constraints, such as  $\ell_1$  regularization (Tibshirani, 1996), to reduce the number of variables and improve interpretability through variable selection. Several sparse methods were proposed and applied to microbiome studies, such as sparse linear discriminant analysis (Clemmensen et al., 2011) and sparse partial least squares discriminant analysis (sPLS-DA, Lê Cao et al., 2016b), but for a single time point. Therefore, further developments are needed to combine time-course modeling with multivariate approaches to start exploring microbial interactions and dynamics.

In addition, current statistical methods have mainly focused on a single microbiome dataset, rather than the combination of different layers of molecular information obtained with parallel multi-omics assays performed on the same biological samples. Data derived from each omics technique are typically studied in isolation and disregard the correlation structure that may be present between the multiple data types. Hence, integrating these datasets enables us to adopt a holistic approach to elucidate patterns of taxonomic and functional changes in microbial communities across time. Some sparse multivariate methods have been proposed to integrate omics and microbiome datasets at a single time point and identify sets of features (multi-omics signatures) across multiple data types that are correlated with one another. For example, Gavin et al. (2018) used the DIABLO method (Singh et al., 2019) to integrate 16S amplicon microbiome, proteomics, and metaproteomics data in a type I diabetes study; Guidi et al. (2016) used sparse PLS (Lê Cao et al., 2008) to integrate environmental and metagenomic data from the Tara Oceans expedition to understand carbon export in oligotrophic oceans, and Fukuyama et al. (2017) used sparse canonical correlation analysis (Witten et al., 2009) to integrate 16S and metagenomic data. However, methods or frameworks

to integrate multiple longitudinal datasets including microbiome data remain incomplete. Zhou et al. (2008) used principal component analysis (PCA) to summarize functional data, with the PC scores used for model fitting, prediction, and inference. However, only pairwise relationships were investigated and for a single type of data. Other type of modeling (loess regression) was used by Ribicic et al. (2018) in combination with sparse PCA to explore the link between chemistry and microbial community data in the biodegradation of chemically dispersed oil, but their approach was not designed to seek for multi-omics signatures.

We propose a computational approach to integrate microbiome data with multi-omics datasets in longitudinal studies. Our framework, described in **Figure 1** includes smoothing splines in a linear mixed model framework to model profiles across groups of samples and builds on the ability of sparse multivariate ordination methods to identify sets of variables highly associated across the data types, and across time. Our framework encompasses data pre-processing, modeling, data clustering, and integration. It is highly flexible in handling one or several longitudinal studies with a small number of time points, to identify groups of taxa with similar behavior over time and posit novel hypotheses about symbiotic relationships, interactions, or competitions in a given condition or environment, as we illustrate in two case studies.

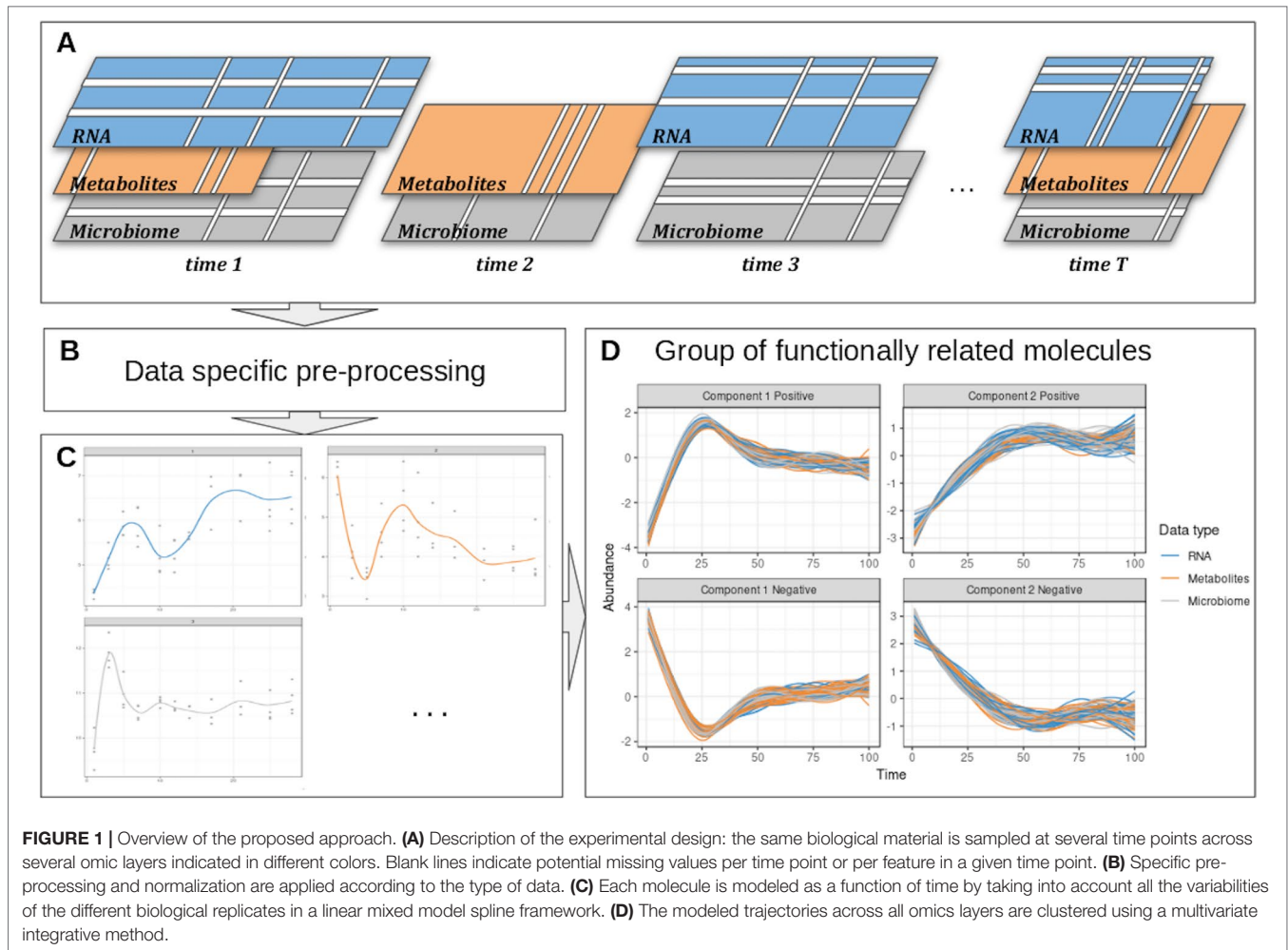
## METHOD

Our proposed approach includes pre-processing for microbiome data, spline modelization within a linear mixed model framework, and a multivariate analysis for clustering and data integration (**Figure 2**).

### Pre-Processing of Microbiome Data

We assume the data are in raw count formats resulting from bioinformatics pipelines such as QIIME (Caporaso et al., 2010) or FROGS (Escudé et al., 2017) for 16S amplicon data. Here, we consider the operational taxonomic unit (OTU) level, but other levels can be considered, as well as other types of microbiome-derived data, such as whole genome shotgun sequencing. The data processing step is described in Lê Cao et al. (2016b) and consists of:

- 1) Low count removal: Only OTUs whose proportional counts exceeded 0.01% in at least one sample were considered for analysis. This step aims to counteract sequencing errors (Kunin et al., 2010).
- 2) Total sum scaling (TSS) can be considered as a “normalization” process to account for uneven sequencing depth across samples. TSS divides each OTU count by the total number of counts in each individual sample but generates compositional data expressed as proportions. Instead, one can use Centered Log Ratio transformation (CLR), that is scale invariant and addresses in a practical way the compositionality issue arising from microbiome data by projecting the data into a Euclidean space (Aitchison, 1982; Fernandes et al., 2014; Gloor et al., 2017). Given a vector  $x$  of  $p$  OTU counts for a given sample, CLR



(eq. 1) is a log transformation of each element of the vector divided by its geometric mean  $G(x)$ :

$$\text{clr}(x) = \left[ \log\left(\frac{x_1}{G(x)}\right), \dots, \log\left(\frac{x_p}{G(x)}\right) \right] \quad (1)$$

where

$$G(x) = \sqrt[p]{x_1 \times x_2 \times \dots \times x_p}$$

## Time Profile Modeling

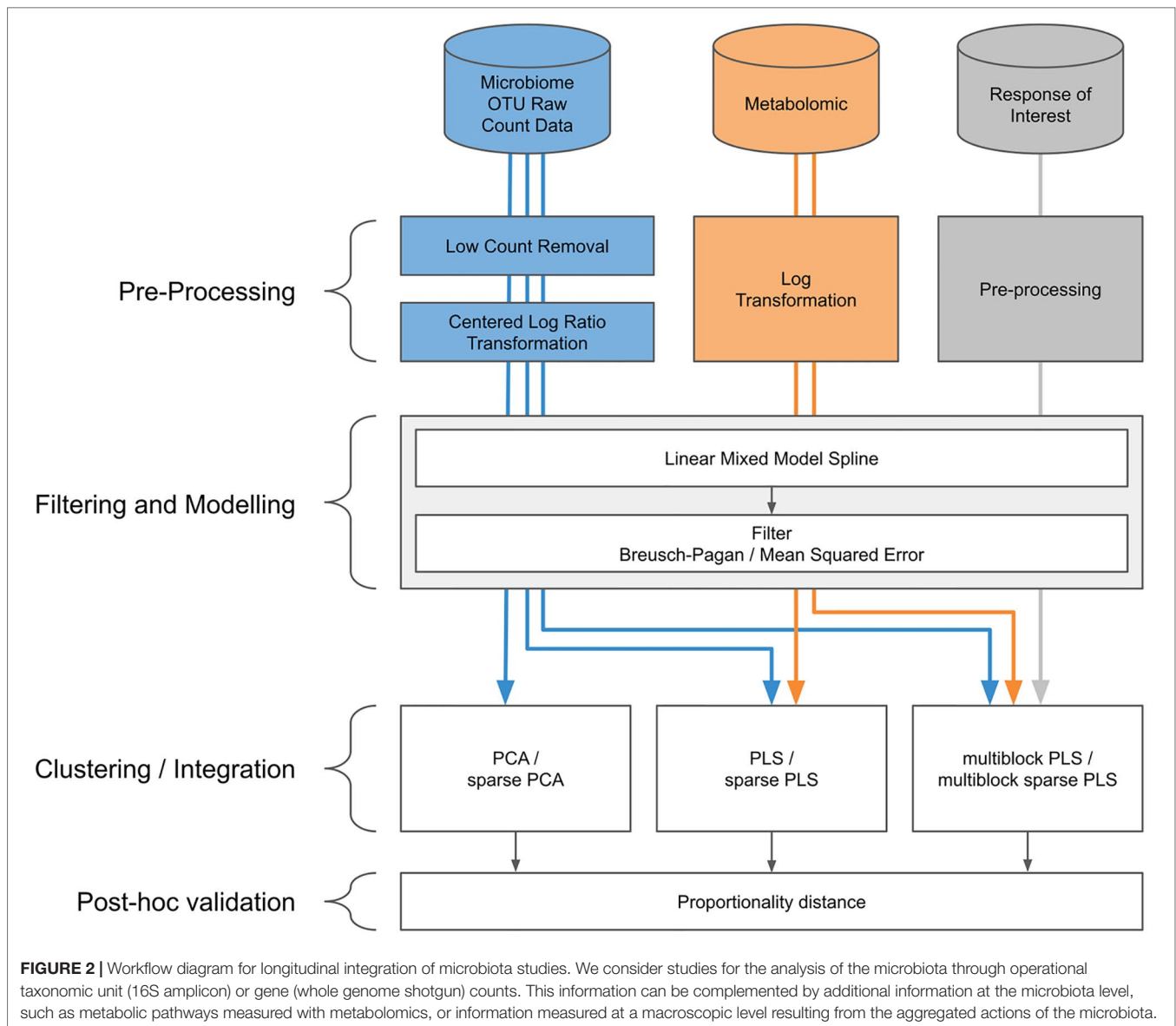
### Linear Mixed Model Splines

The linear mixed model spline (LMMS) modeling approach proposed by Straube et al. (2015) takes into account between and within individual variability and irregular time sampling. LMMS is based on a linear mixed model representation of penalized splines (Durbán et al., 2005) for different types of models. Through this flexible approach of serial fitting, LMMS

avoids under- or over-smoothing. Briefly, four types of models are consecutively fitted in our framework on the CLR data:

- (1) A simple linear regression of taxa abundance on time, estimated *via* ordinary linear least squares—a straight line that assumes the response is not affected by individual variation
- (2) A penalized spline proposed by Durbán et al. (2005) to model nonlinear response patterns
- (3) A model that accounts for individual variation with the addition of a subject-specific random effect to the mean response in model (2)
- (4) An extension to model (3) that assumes individual deviations are straight lines, where individual-specific random intercepts and slopes are fitted

All four models are described in **Appendix 1**. Straube et al., 2015 showed that the proportion of profiles fitted with the different models increased in complexity with the organism considered. Different types of splines can be considered in models (2)–(4), including a cubic spline basis (Verbyla et al., 1999), a penalized spline and a cubic penalized spline. A cubic spline basis uses all inner time points of the measured time



interval as knots and is appropriate when the number of time points is small ( $\leq 5$ ), whereas the penalized spline and cubic penalized spline bases use the quantiles of the measured time interval as knots; see Ruppert (2002). In our case studies, we used penalized splines. The LMMS models are implemented in the R package `lmms` (Straube et al., 2016).

### Prediction and Interpolation

The fitted splines enable us to predict or interpolate time points that might be missing within the time interval (e.g., inconsistent time points between different types of data or covariates). Additionally, interpolation is useful in our multivariate analyses described below to smooth profiles, and when the number of time points is small ( $\leq 5$ ). In the following section, we therefore consider data matrices  $X$  ( $T \times P$ ), where  $T$  is the number of (interpolated) time points and  $P$  the number of taxa. The individual dimension has thus been summarized through the

spline fitting procedure, so that our original data matrix of size ( $N \times P \times T$ ), where  $N$  is the number of biological samples, is now of size ( $T \times P$ ).

### Filtering Profiles After Modeling

A simple linear regression model (1) might be the result of highly noisy data. To retain only the most meaningful profiles, the quality of these models was assessed with a Breusch–Pagan test to indicate whether the homoscedasticity assumption of each linear model was met (Breusch and Pagan, 1979) simple. We also used a threshold based on the mean squared error (MSE) of the linear models, by only including profiles for which their MSE was below the maximum MSE of the more complex fitted models (2)–(4). The latter filter was only applied when a large number of linear models (1) were fitted and the Breusch–Pagan test was not considered stringent enough.

## Clustering Time Profiles

### Principal Component Analysis and Sparse Principal Component Analysis

Multivariate dimension reduction techniques such as PCA (Jolliffe, 2011) and sparse PCA (Huang and Zheng, 2006) can be used to cluster taxa profiles. To do so, we consider as data input the  $X$  ( $T \times P$ ) spline fitted matrix. Let  $t_1, t_2, \dots, t_H$  denote the  $H$  principal components of length  $T$  and their associated  $v_1, v_2, \dots, v_H$  factors—or loading vectors, of length  $P$ . For a given PCA dimension  $h$ , we can extract a set of strongly correlated profiles by considering taxa with the top absolute coefficients in  $v_h$ . Those profiles are linearly combined to define each component  $t_h$ , and thus, explain similar information on a given component. Different clusters are therefore obtained on each dimension  $h$  of PCA,  $h = 1 \dots H$ . Each cluster  $h$  is then further separated into two sets of profiles which we denote as “positive” or “negative” based on the sign of the coefficients in the loading vectors (see Results section).

A more formal approach can be used with sparse PCA. Sparse PCA includes  $\ell_1$  penalizations on the loading vectors to select variables that are keys for defining each component and are highly correlated within a component (see Huang and Zheng, 2006 for more details).

### Choice of the Number of Clusters in Principal Component Analysis

We propose to use the average silhouette coefficient (Rousseeuw, 1987) to determine the optimal number of clusters, or dimensions  $H$ , in PCA. For a given identified cluster and observation  $I$ , the silhouette coefficient of  $I$  is defined as

$$s(i) = \frac{b(i) - a(i)}{\max(a(i), b(i))} \quad (5)$$

where  $a(i)$  is the average distance between observation  $i$  and all other observations within the same cluster, and  $b(i)$  is the average distance between observation  $i$  and all other observations in the nearest cluster. A silhouette score is obtained for each observation and averaged across all silhouette coefficients, ranging from  $-1$  (poor) to  $1$  (good clustering).

We adapted the silhouette coefficient to choose the number of components or clusters in PCA and sparse PCA (sPCA, i.e.,  $2 \times H$  clusters), as well as the number of profiles to select for each cluster. Each observation in Eq. (5) now represents a fitted LMMS profile, and the distance between two profiles is calculated using the Spearman correlation coefficient.

Within a given cluster, we calculate the silhouette coefficient of each LMMS profile and apply the following empirical rules for cluster assignment: a coefficient  $> 0.5$  assigns the profile to the cluster, and a value between  $0$  and  $0.5$  indicates an uncertain assignment as the profile can be assigned to one or two clusters, while a negative value indicates that the profile should not be assigned to this particular cluster.

To choose the appropriate number of profiles per sPCA component, we perform as follows: for each component, we set a grid of the number of profiles to be retained with

sPCA and calculated the average silhouette coefficient per cluster (there are two clusters per component). The final number of profiles to select is arbitrarily set when we observe a sudden decrease in the average silhouette coefficient (see Results section).

### Comparison With Functional Principal Component Analysis

Functional principal component analysis (fPCA) has been widely used to cluster longitudinal data by decomposing data matrices into temporal variation models (Hyndman and Ullah, 2007) and has been used in several biological applications (Silverman et al., 1996; Yao et al., 2005). fPCA first models longitudinal profiles into a finite basis of functions then clusters the longitudinal profiles using the basis expansion coefficients of the fPCA scores. fPCA requires the user to choose the number of clusters and the number of components—based on Akaike information criterion, Bayesian information criterion, or percentage of total explained variance, the approach to estimate the fPCA scores—based on conditional expectation or numerical integration, and to cluster the profiles. We used the “fdapace” R package that includes two types of clustering methods, based on model-based clustering of finite mixture Gaussian distribution (“EMCluster”) or k-means algorithm based on the fPCA scores.

### Evaluation Clustering

We can assess the quality of clustering with internal measures such as compactness (Dunn, Rand indices, and Jaccard index) or cluster separation. For the latter case, the silhouette coefficient is recognized as an informative criterion Wang et al. (2009) and can be used to compare several clustering results based on the same data. Thus, we used this criterion to assess different methods (PCA, sPCA, and fPCA), or to assess the same method with different parameters—for example, to identify the appropriate number of clusters as we described in 2.4.2. The best clustering approach yields the highest silhouette coefficient.

### Measure of Association for Compositional Data

Compositional data arise from any biological measurement made based on relative abundance (Lovell et al., 2015; Gloor et al., 2017). Microbiome data in particular are compositional for several reasons, including biological, technical, and computational. Thus, interpretation based on correlations between profiles must be made with caution as it is highly likely to be spurious. Proportional distances have been proposed as an alternative to measure association. The compositional data analysis field is an active field of research, but methods are critically lacking for longitudinal data. Here, we adopt a practical and *post hoc* approach to evaluate pairwise associations of microbial and omics profiles once they have been assigned to their clusters. We used the proportionality distance  $\phi_s$  proposed by Lovell et al. (2015) and implemented in the “propr” R package (Quinn et al., 2017). For two LMMS

profiles  $x_i$  and  $x_j$ , we define the pairwise proportionality distance as

$$\varphi_s(x_i, x_j) = \frac{\text{var}(x_i - x_j)}{\text{var}(x_i + x_j)}. \quad (6)$$

A small value indicates that, in proportion, the pair of profiles is strongly associated. We calculated the distance  $\varphi_s$  on the log-transformed LMMS modeled profiles within each identified cluster to exclude potentially spurious correlations and further guide the interpretation of the results. In addition, to evaluate the quality of our clustering approach, we compared the pairwise distances of the profiles within a particular cluster and profiles outside the cluster.

## Integration

### Multiblock Projection to Latent Structures Methods

To integrate multiple datasets (also called *blocks*) measured on the same biological samples, we used multivariate methods based on projection to latent structures (PLS) methods (Wold, 1975), which we broadly term *multiblock PLS* approaches. For example, we can consider generalized canonical correlation analysis (GCCA, Tenenhaus and Tenenhaus, 2011; Tenenhaus et al., 2014), which, contrary to what its name suggests, generalizes PLS for the integration of more than two datasets. Recently, we have developed the DIABLO method to discriminate different phenotypic groups in a supervised framework (Singh et al., 2019). In the context of this study, however, we present the sparse GCCA in an unsupervised framework, where input datasets are spline-fitted matrices.

We denote  $Q$  data sets  $X^{(1)}(TxP_1)$ ,  $X^{(2)}(TxP_2)$ , ...,  $X^{(Q)}(TxP_Q)$  measuring the expression levels of  $P_q$  variables of different types (taxa, "omics," continuous response of interest), modeled on  $T$  (interpolated) time points,  $q = 1, \dots, Q$ . GCCA solves for each component  $h = 1, \dots, H$ :

$$\begin{aligned} \max_{a_h^{(1)}, \dots, a_h^{(Q)}} \sum_{q,j=1, q \neq j}^Q c_{q,j} \text{cov}(X_h^{(q)} a_h^{(q)}, X_h^{(j)} a_h^{(j)}), \\ \text{s.t. } \|a_h^{(q)}\|_2 = 1 \text{ and } \|a_h^{(q)}\|_1 \leq \lambda^{(q)} \end{aligned} \quad (7)$$

where  $\lambda^{(q)}$  is the  $\ell_1$  penalization parameter,  $a_h^{(q)}$  is the loading vector on component  $h$  associated with the residual (deflated) matrix  $X_h^{(q)}$  of the data set  $X^{(q)}$ , and  $C = \{c_{qj}\}$  is the design matrix.  $C$  is a  $Q \times Q$  matrix that specifies whether datasets should be correlated and includes values between zero (datasets are not connected) and one (datasets are fully connected). Thus, we can choose to take into account specific pairwise covariances by setting the design matrix (see Rohart et al., 2017 for implementation and usage) and model a particular association between pairs of datasets, as expected from prior biological knowledge or experimental design. In our integrative case study, we used sparse PLS, a special case of Eq. (7) to integrate

microbiome and metabolomic data, as well as sparse multiblock PLS to also integrate variables of interest. Both methods were used with a fully connected design.

The multiblock sparse PLS method was implemented in the `mixOmics` R package where the  $\ell_1$  penalization parameter is replaced by the number of variables to select, using a soft-thresholding approach (see more details in Rohart et al., 2017).

### Parameter Tuning

The integrative methods require choosing the number of components  $H$ , defined as  $t_h^{(q)} = X_h^{(q)} a_h^{(q)}$ , and number of profiles to select on each PLS component and in each dataset. We generalized the GCCA approach by using the silhouette coefficient based on a grid of parameters for each dataset and each component.

## Simulation and Case Studies

### Simulation Study Description

A simulation study was conducted to evaluate the clustering performance of multivariate projection-based methods such as PCA, and the ability to interpolate time points in LMMS.

Twenty reference time profiles were generated on nine equally spaced time points and assigned to four clusters (five profiles each). These ground truth profiles were then used to simulate new profiles. We generated 500 simulated datasets.

### Clustering Performance

We first compared profiles simulated then modeled with or without LMMS:

- For each of the reference profiles, five new profiles (corresponding to five individuals) were sampled to reflect some inter-individual variability as follows: let  $x$  be the observation vector for a reference profile  $r$ ,  $r = 1 \dots 20$ ; for each time point  $t$  ( $t = 1, \dots, 9$ ), five measurements were randomly simulated from a Gaussian distribution with parameters  $\mu = x_{t,r}$  and  $\sigma^2$ , where  $\sigma = \{0, 0.1, 0.2, 0.3, 0.4, 0.5, 1, 1.5, 2, 3\}$  to vary the level of noise. This noise level was representative of the data described below. The profiles from the five individuals were then modeled with LMMS, resulting in 500 matrices of size  $(9 \times 20)$  for each level of noise  $\sigma$ .
- For each of the reference profiles, one new profile was simulated as described in step A, but no LMMS modeling step was performed, resulting in 500 matrices of size  $(9 \times 20)$  for each level of noise  $\sigma$ .

Clustering was obtained with PCA and compared to the reference cluster assignments in a confusion matrix.

The clustering was evaluated by calculating the accuracy of assignment ( $\frac{TP + TN}{TP + FP + TN + FN}$ ) from the confusion matrix, where for a given cluster, TP (true positive) is the number of profiles correctly assigned in the cluster, FN (false negative) is the number of profiles that have been wrongly assigned to another cluster, TN (true negative) is the number of profiles correctly assigned to another cluster, and FP (false positive) is the number

of profiles incorrectly assigned to this cluster. Besides accuracy, we also calculated the Rand index (Rand, 1971) objective as a similarity metric to the clustering performance of PCA. The clustering results from fPCA were poor, even for a low level of noise (**Supplementary Figure 1**); thus, fPCA was not compared against PCA.

### Interpolation of Missing Time Points

To evaluate the ability of LMMS to predict the value of a missing time point for a given feature over time, we randomly removed 0 to 4 measurement points in the simulated datasets described above in step A. We compared the PCA clustering performance with or without LMMS interpolation.

### Infant Gut Microbiota Development

The gastrointestinal microbiome of 14 babies during the first year of life was studied by Palmer et al. (2007). The authors collected an average of 26 stool samples from healthy full-term infants. As infants quickly reach an adult-like microbiota composition, we focused our analyses on the first 100 days of life. Infants who received an antibiotic treatment during that period were removed from the analysis, as antibiotics can drastically alter microbiome composition (Dudek-Wicher et al., 2018).

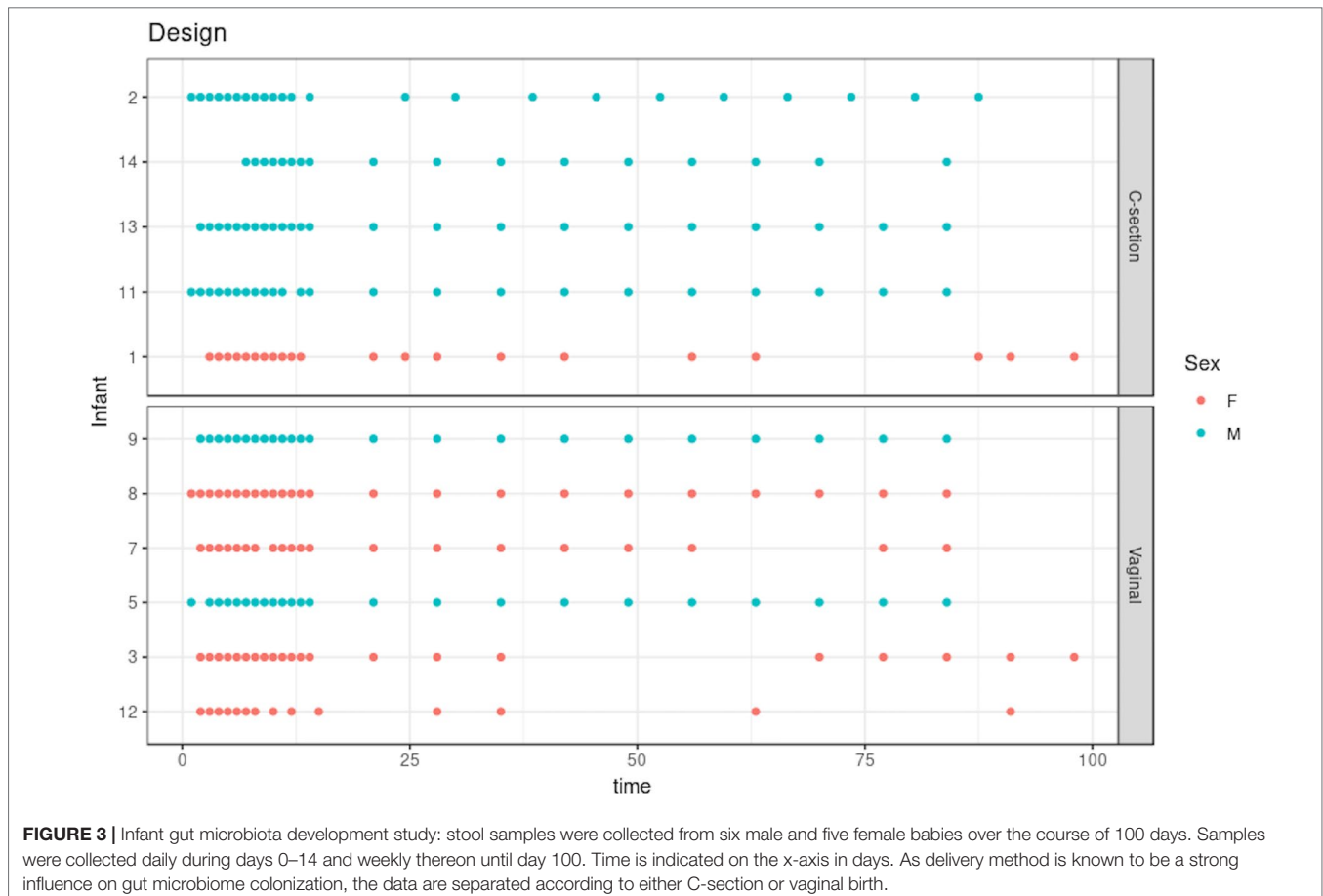
The dataset we analyzed included 21 time points on average for 11 selected infants (vaginal delivery = 6, C-section = 5;

see **Figure 3**). Samples were collected daily during days 0–14 and weekly after the second week. We separated our analyses based on the delivery mode (C-section or vaginal), as this is known to have a strong impact on gut microbiota colonization patterns and diversity in early life Rutayisire et al. (2016). The purpose of our statistical analysis was to identify a bacterial signature that describes the dynamics of a baby's microbial gut development in the first days of life, as well as compare differences in signatures between babies born by vaginal delivery or by C-section. As this study is single omics, we applied our framework depicted in **Figure 2** with sPCA.

### Waste Degradation Study

Anaerobic digestion (AD) is a highly relevant microbial process to convert waste into valuable biogas. It involves a complex microbiome that is responsible for the progressive degradation of molecules into methane and carbon dioxide. In this study, AD's biowaste was monitored across time (more than 150 days) in three lab-scale bioreactors as described in (Poirier et al., 2016).

We focused our analysis on days 9 to 57, which correspond to the most intense biogas production. Degradation performance was monitored through four parameters: methane and carbon dioxide production (16 time points) and the accumulation of



acetic and propionic acid in the bioreactors (5 time points). Microbial dynamics were profiled with 16S RNA gene metabarcoding as described in Poirier et al. (2016) and included 4 time points and 90 OTUs. A metabolomic assay was conducted on the same biological samples at four time points with gas chromatography coupled to mass spectrometry GC-MS after solid phase extraction to monitor substrates degradation (Limam et al. (2010)). The XCMS R package (version 1.52.0) was used to process the raw metabolomics data (Smith et al., 2006). GC-MS analyses focused on 20 peaks of interest identified by the National Institute of Standards and Technology database. Data were then log-transformed. The purpose of the study was to investigate the relationship between biowaste degradation performance and microbial and metabolomic dynamics across time. The aim of our statistical analysis was to identify highly associated multi-omic signatures characterizing waste degradation dynamics in the three bioreactors. This study involves the integration of two omics datasets and degradation performance measures; thus, we applied sPLS and multiblock sPLS, as shown in our workflow in **Figure 2**.

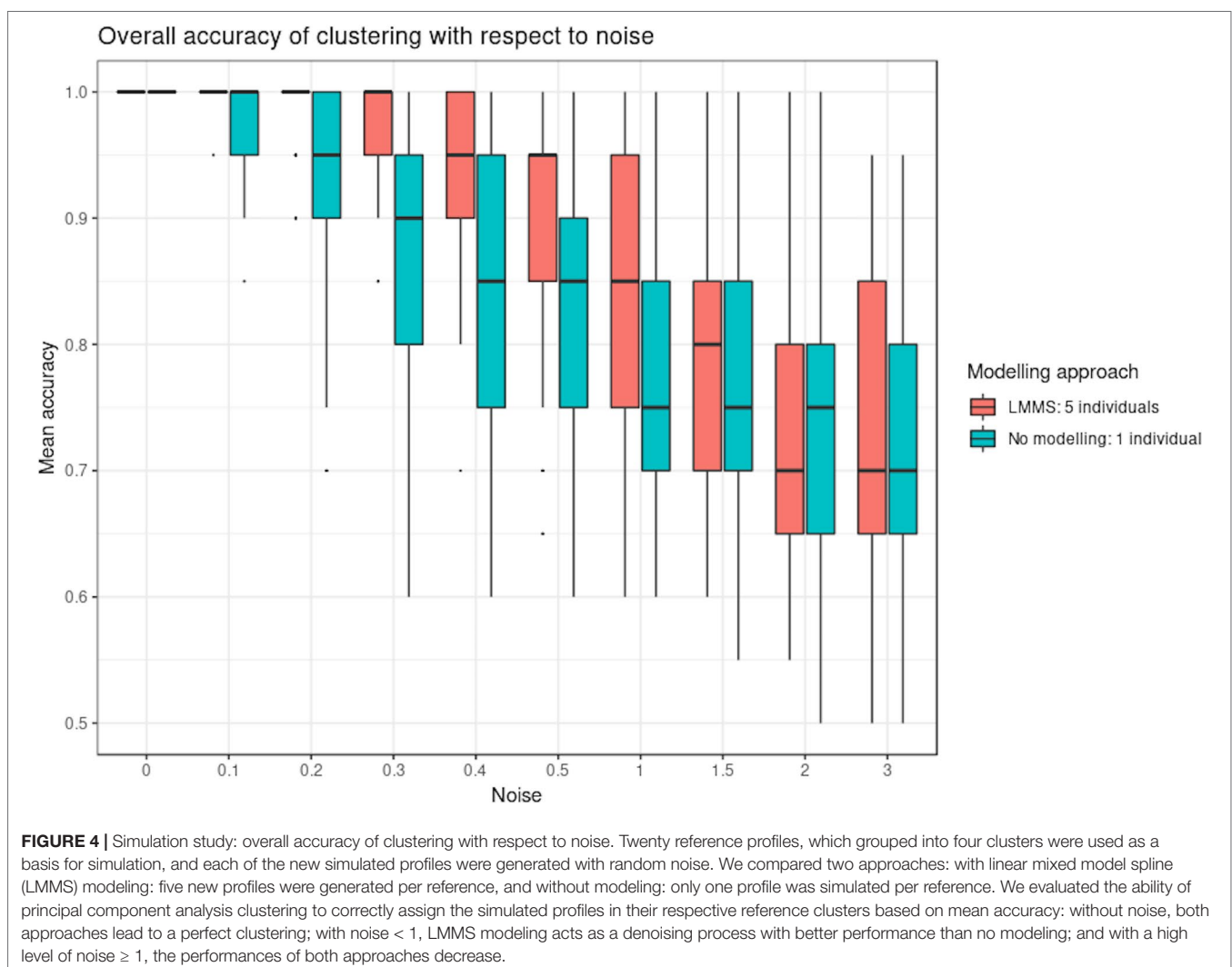
## RESULTS

### Simulation Study Clustering Performance

**Figure 4** shows the clustering performance of PCA with an increasing amount of noise in the simulated profiles. Unsurprisingly, PCA gave optimal clustering performance when noise was absent, with or without profile modeling to take into account individual variability. When noise increased, PCA performed better with modeling, which acts as a denoising process. Finally, a high level of noise showed the limitation of the modeling approach, as similar clustering results were obtained with or without LMMS modeling. However, the PCA clustering performance was still very good, with a mean accuracy of 0.7 when the level of noise was maximum.

### Interpolation of Missing Time Points

We evaluated the ability of LMMS to interpolate an increasing number of missing time points (up to four). Interpolation is important in our framework as it allows the estimation of evenly spaced time points as well as time points that may be missing in





one data set but not in the other (e.g., biowaste degradation study). Interpolation did not seem to affect the clustering performance of PCA (Figure 5 and Supplementary Figure 2). Rather, the level of noise had the largest impact on clustering: the mean accuracy was close to 1 when the noise was nonexistent but decreased as the number of missing time points and noise increased. In the latter scenarios, LMMS interpolation seemed to give, on average, better clustering than without interpolation. When the number of missing time points increased, we observed a better classification accuracy with noise compared to no noise. This can be explained by the LMMS modeling of straight lines in the latter case that led to poor clustering (Supplementary Figure 3).

## Clustering Time Profiles: Infant Gut Microbiota Development Study Pre-Processing and Modeling

A total of 2,149 taxa were identified in the raw data (Table 1). After the pre-processing steps illustrated in Figure 2, a smaller number of OTUs were found in fecal samples of babies born by C-section than vaginal delivery. Similarly, a simple linear regression model showed a smaller proportion of OTUs in babies born *via* C-section (73%) than vaginal delivery (81%), and this was also observed after the filtering step (Table 1).

## Comparison of Principal Component Analysis and Functional Principal Component Analysis

According to our tuning criteria, we obtained four clusters with PCA (i.e., two components). We therefore set the same number

**TABLE 1** | Infant gut microbiota development study: number of operational taxonomic units (OTUs) identified and linear model types fitted according to delivery mode.

	C-section	Vaginal
Identified OTUs	2,149	2,149
Number of OTUs after pre-processing	107	117
Linear model types	(1) 78 (2) 29	95 22
Linear model types after filtering	(1) 42 (2) 29	68 22

of clusters in fPCA for comparative purposes. PCA clustering outperformed fPCA for each delivery mode dataset that was analyzed (see Table 2). The resulting fPCA clustering is displayed in Figure 6 for babies born *via* vaginal delivery. We found that the EM approach in fPCA tended to cluster a larger number of uncorrelated OTUs compared to the *k*-CFC approach (average silhouette coefficient = 0.07 for EM and 0.61 for *k*-CFC).

We used sPCA to select key OTU profiles for each cluster. This step is essential for discarding profiles that are distant from the

**TABLE 2** | Infant gut microbiota development study: average silhouette coefficient according to clustering method.

	PCA	sPCA	fPCA ( <i>k</i> -CFC)	fPCA(EM)
Vaginal	0.84	0.95	0.61	0.07
C-section	0.87	0.86	0.69	0.35

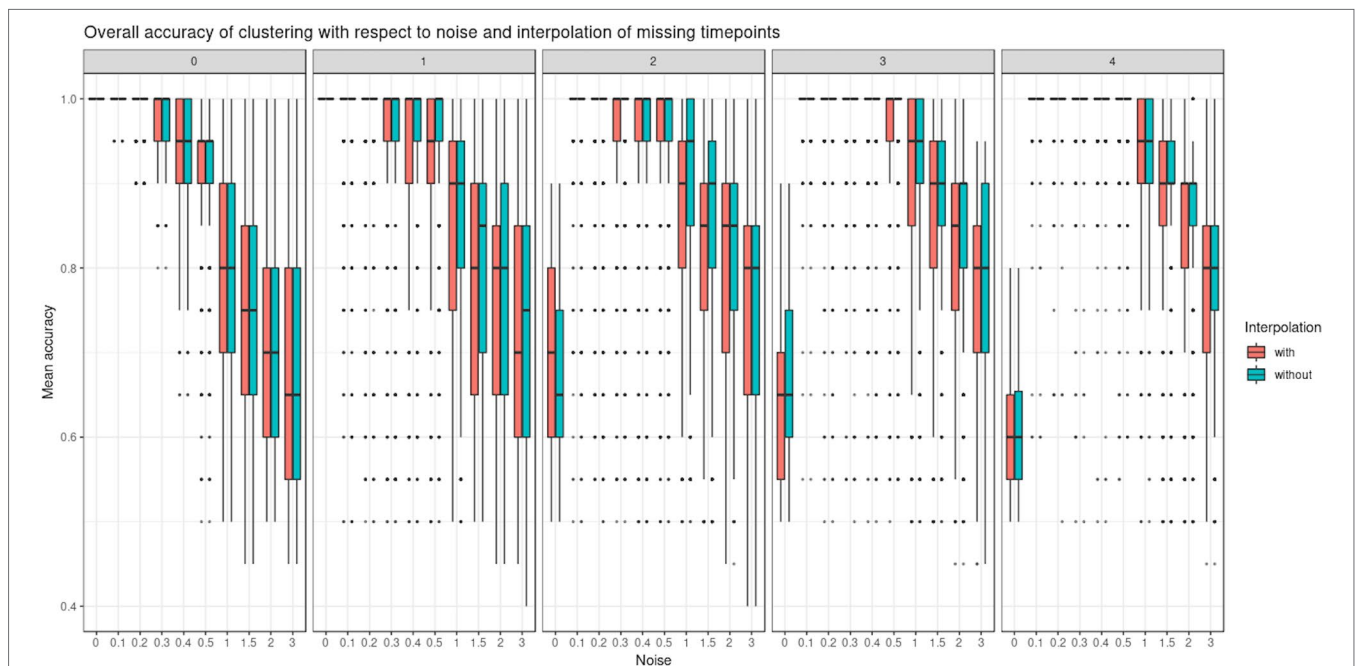
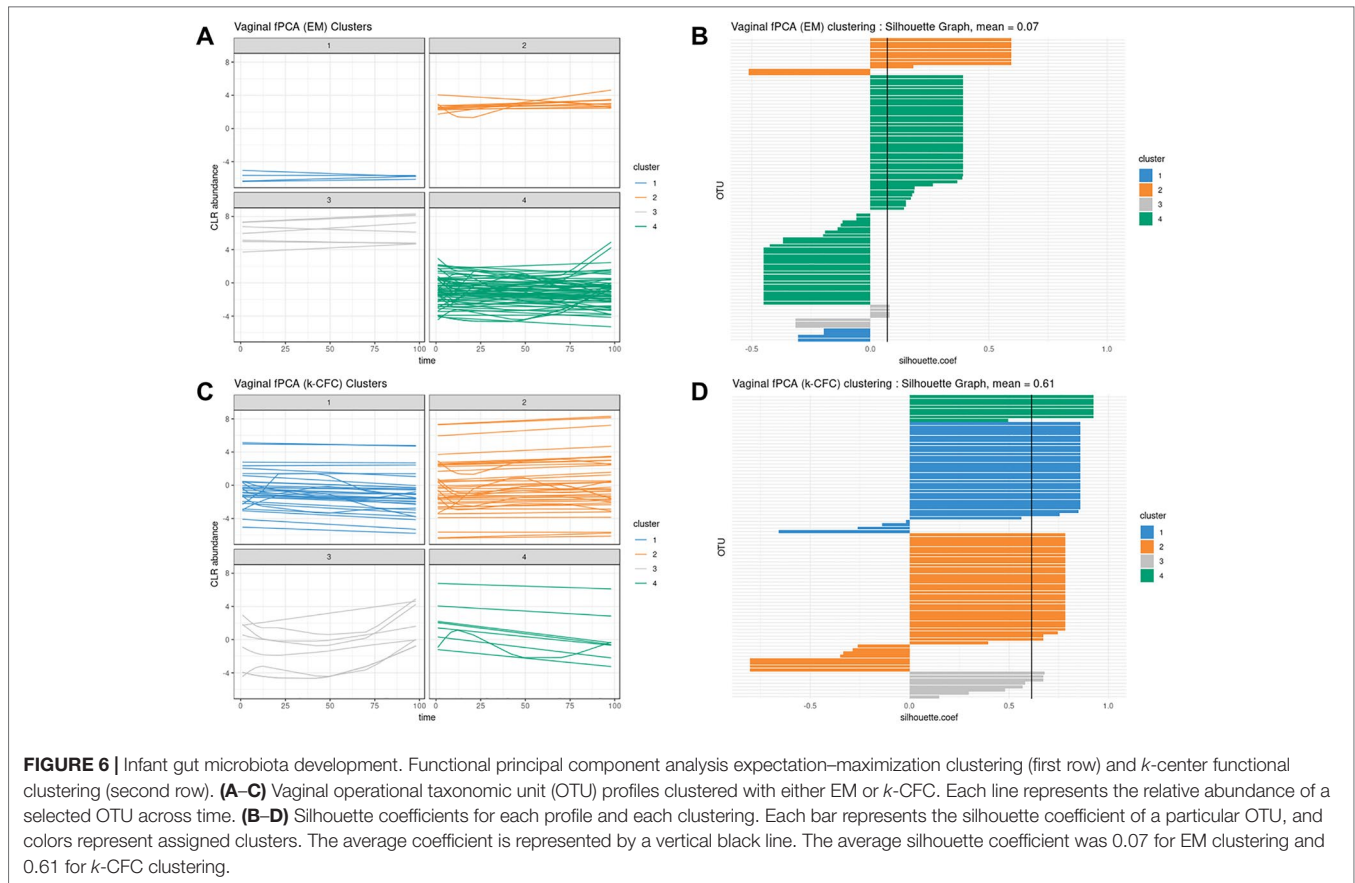


**FIGURE 5** | Simulated study: overall accuracy of clustering when time points are missing. The simulation scheme is described in 2.7.1; however, here, some time points were removed. We compared the ability of linear mixed model spline (LMMS) to interpolate missing time points. When there are no time points missing, both interpolated and non-interpolated approaches gave a similar performance. When the number of time points increases, the classification accuracy decreases. Without noise and with several time points removed, LMMS tended to model straight lines, resulting in poor clustering (see also Supplementary Figure 3).

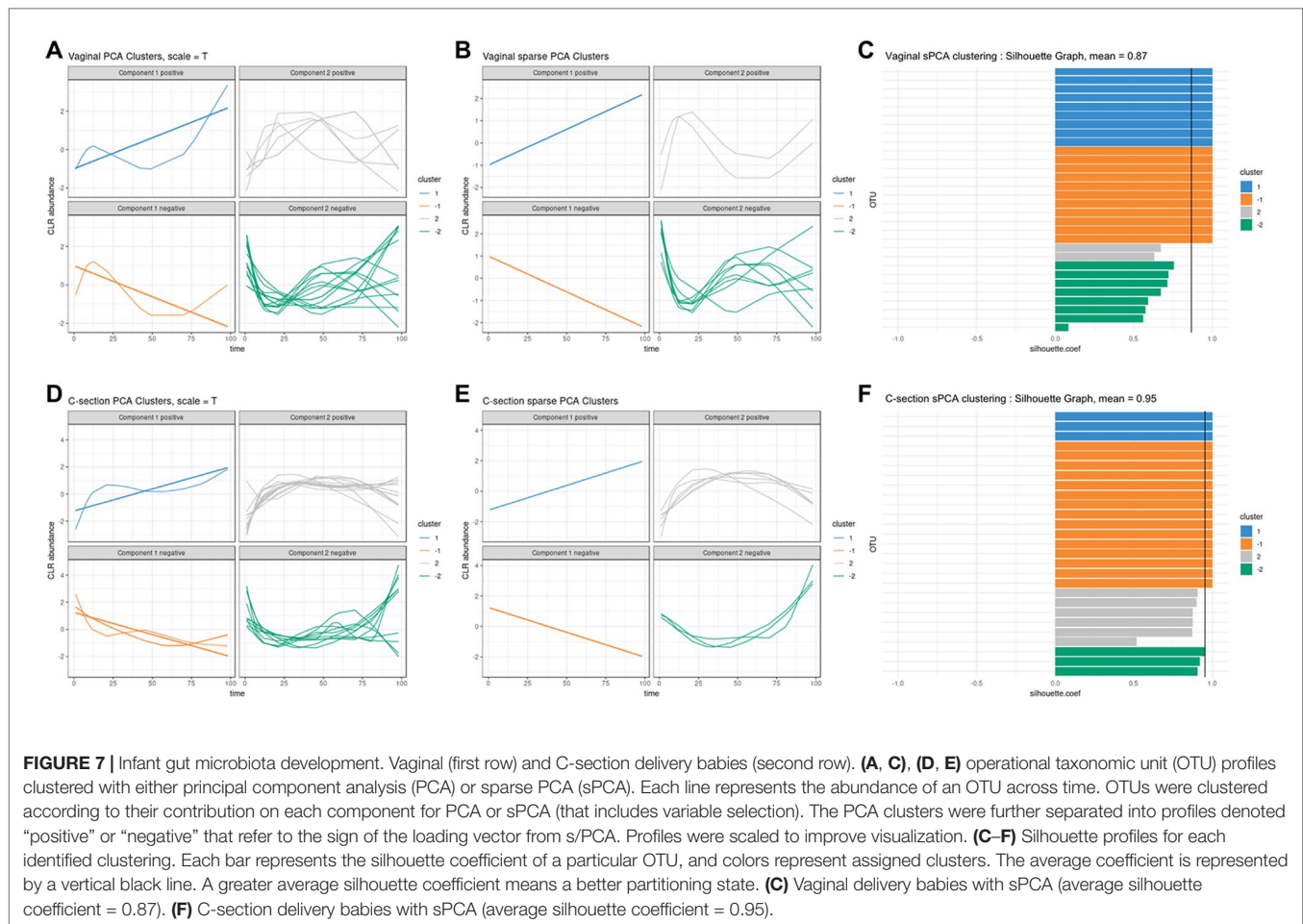


average cluster profile and thus not informative. As expected, we observed an overall increase in the silhouette average coefficient for the sPCA clustering compared to PCA, indicating a better clustering capability (see **Table 2**). According to the silhouette average coefficient, vaginal delivery showed the best partitioning for PCA clustering (0.87; **Table 2**). Cluster 1 (denoted “component 1 positive” in **Figure 7A**) showed a relative increase in abundance of species, including some that are characteristic of a healthy “adult-like” gut microbiome composition such as the clade *Bacteroidetes* (Thursby and Juge, 2017). The proportionality distance within cluster 1 was low (**Supplementary Table 1**), with a strong association between *Bacteroides* and *Fusobacteria* ( $\varphi_s = 0.04$ ), as well as between *Actinobacter* with *Bacteroides* ( $\varphi_s = 0.02$ ) and *Fusobacteria* ( $\varphi_s = 0.09$ ). According to this distance, there might have been a spurious correlation identified between the genus *Bacteroides* and an environmental uncultured bacterium (clone *HuCA36*) ( $\varphi_s = 14.81$ ); see **Supplementary Table 2**. In cluster 2 (“component 1 negative”), relative profile abundance tended to decrease and corresponded to genera found in vaginal and skin microbiota, such as *Lactobacillus* and *Propionibacterium* (Grice and Segre, 2011; Bing et al., 2012). According to the proportionality distance, *Propionibacterium* and *Lactobacillus* were highly associated ( $\varphi_s = 0.29$ ) as well as with *Campylobacter* ( $\varphi_s = 0.39$ , see **Supplementary Table 2**). Clusters 3 and 4 (denoted “component 2 positive and negative”) highlighted taxa profiles with negative association.

A cladogram representing all OTUs and those selected by sPCA for each cluster is shown in **Figure 8** and illustrates that most families are presented in our OTU selection. In addition, we can observe specific clusters—family patterns as discussed above.

Thus, with this preliminary PCA analysis, we were able to rebuild a partial history behind the development of the gut microbiota. Vaginal species that initially colonized in the gut progressively disappeared to enable species that characterize adult gut microbiota.

For babies born by C-section, four clusters were identified by PCA (**Figure 7D**; cladogram visualization is available in **Supplementary Figure 4**). The median values of the proportionality distance within the different clusters were significantly lower than between the selected OTUs in the clusters and all the other OTUs (**Supplementary Table 3**). For example, the median value within cluster 1 was 0.11 compared to 1.36 outside the cluster. Clusters 1 and 2 (“component 1 positive and negative”) displayed either an increase or decrease in relative abundance. However, none of the cluster 2 species are known to characterize, or were found in, vaginal delivery, suggesting that the infant gut was first colonized by the operating room microbes as already demonstrated by Shin et al. (2015). Cluster 3 (“component 2 positive”) revealed transitory states of increase then decrease of relative abundance profiles, while cluster 4 (“component 2 negative”) showed the reverse trend.



When comparing the dynamics of the two delivery methods, we found a higher diversity in the intestinal microbiota of babies born vaginally (117 modeled profiles) than by C-section (107). For vaginal delivery, the modeling step identified a larger proportion of straight lines, which may indicate a greater inter-individual variability compared to C-section delivery. The clusters denoted “component 1 positive” in both delivery modes showed an increased relative abundance over time, with 32 OTUs assigned to this cluster in vaginally born babies, compared to 11 in C-section (Table 3). Despite the relatively sterile environment of the operating room, it was surprising to observe similar number of OTUs in cluster “component 1 negative” for both types of delivery mode (vaginal: 38, C-section: 35), as we would have expected to identify a larger number of opportunistic microorganisms colonizing babies born vaginally (e.g., *Propionibacterium acnes*, *Campylobacter*). These include species found on the surface of the skin and in the vaginal flora. However, for babies born by C-section, we observed a large number of microorganisms from various origins (e.g., *Staphylococcus*, *Rickettsia*, *Rhodobacter*).

In summary, sparse PCA clustering of LMMS modeled profiles enabled the identification of groups of microorganisms with relative increased abundance over time. These microorganisms are characteristics of an adult gut microbiota. We also identified

groups of opportunistic microorganisms with a decreasing relative abundance over time. We also found that, during the first year of life, gut microbiota was more diverse for babies born by vaginal than C-section delivery.

### Clustering Omics: Waste Degradation Study Pre-Processing and Modeling

A total of 90 OTUs were identified in the 12 samples of the initial dataset (Table 4). After pre-processing, 51 OTUs were retained. Approximately 60% (resp. 50%) of the OTUs (resp. metabolites) were fitted with linear regression models (1), and 40% (resp. 50%) were modeled by more complex spline models (2)–(4). All performance measures were also modeled by splines. During the filtering step, seven OTUs and four metabolites that were fitted with linear regression models were discarded. The small number of profiles that were filtered out indicated that the variability between the three bioreactors was relatively low.

### Sparse PCA on Concatenated Datasets

As a first and naive attempt to jointly analyze microbial, metabolomic, and performance measures, all three datasets were concatenated

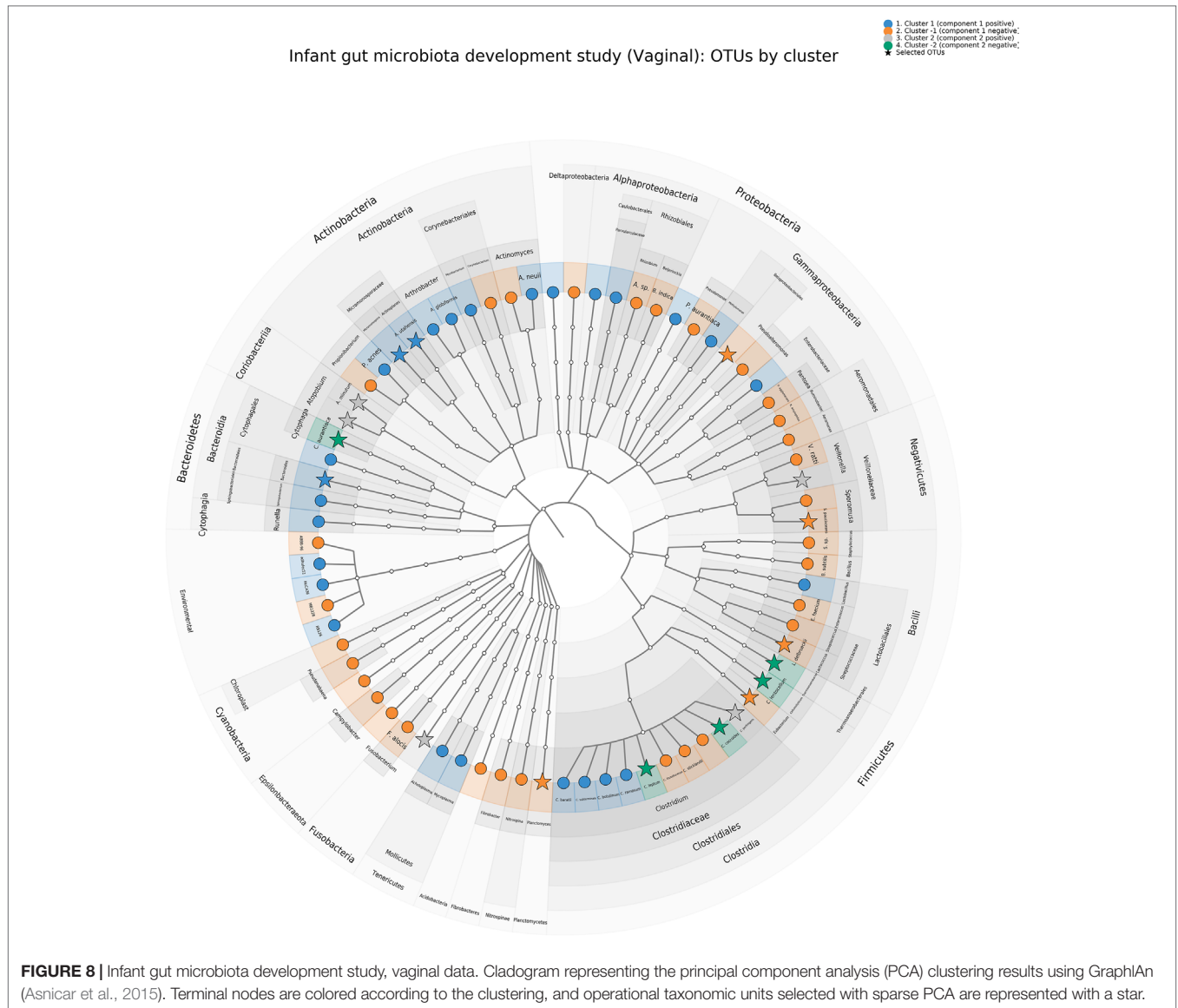


**FIGURE 8 |** Infant gut microbiota development study, vaginal data. Cladogram representing the principal component analysis (PCA) clustering results using GraphlAn (Asnicar et al., 2015). Terminal nodes are colored according to the clustering, and operational taxonomic units selected with sparse PCA are represented with a star.

then analyzed with sPCA. Only a very small number of profiles from the different datasets were selected. This small selection is likely due to the high variability in each data type. Selected variables included mainly OTUs and performance measures. These were assigned to four clusters and included respectively 1, 3, 2, and 3 OTUs with 0, 1, 2, and 0 metabolites and 2, 0, 1, and 0 performance measures. The average silhouette coefficient was 0.744, a potentially sub-optimal clustering compared to our analyses presented in the next section. This preliminary investigation highlighted the limitation of sPCA to identify a sufficient number of associated profiles from disparate sources.

**Microbiome-Metabolomic Integration With sPLS**

The results from the sPLS analysis are shown in **Supplementary Figure 5**. Four clusters of variables were identified, and the average silhouette coefficient of 0.954 confirmed that sPLS led to better clustering of the different types of profiles than sPCA. The

**TABLE 3 |** Infant gut microbiota development study: number of operational taxonomic units (OTUs) per cluster identified with principal component analysis (PCA) clustering and OTUs selected in brackets with sparse PCA.

	C-section	Vaginal
Cluster 1 (comp 1 positive)	11 (3)	32 (9)
Cluster 2 (comp 1 negative)	35 (15)	38 (11)
Cluster 3 (comp 2 positive)	15 (6)	6 (2)
Cluster 4 (comp 2 negative)	10 (3)	14 (8)

proportionality distances of the profiles within each cluster are presented in **Table 5** and in **Supplementary Figure 6**. Their low values indicated strong associations between profiles within each cluster, compared to any association outside each of the clusters. A cladogram representing the selected OTUs only, according to each sPLS cluster is shown in **Supplementary Figure 7**.

The first cluster (denoted “component 1 negative”) included 10 OTUs and 4 metabolite variables and showed increasing

**TABLE 4 |** Waste degradation study: operational taxonomic units (OTUs), metabolites, and performance modeling and filtering in the bioreactor study. Only OTU data were pre-processed.

Type of features		OTUs	Metabolites	Performance
Number of features		90	20	4
Number of Features after pre-processing		51	NA	NA
Linear model types	(1)	30	10	0
	(2)	19	0	2
	(3)	2	4	0
	(4)	0	6	2
Linear model types after filtering	(1)	24	6	0
	(2)	19	0	2
	(3)	2	4	0
	(4)	0	6	2

**TABLE 5 |** Waste degradation study: proportionality distance for clusters identified with sparse PLS. The median distance between all pairs of profiles, within cluster, and with the entire background set (outside a given cluster) is reported. A Wilcoxon test p-value assesses the difference between the medians.

Cluster	Median within cluster	Median outside cluster	Wilcoxon test P-value
1 (comp 1 positive)	0.43	1.37	$9.40 \times 10^{-57}$
-1 (comp 1 negative)	0.42	1.11	$1.76 \times 10^{-28}$
2 (comp 2 positive)	0.29	0.97	$5.71 \times 10^{-24}$
-2 (comp 2 negative)	0.01	0.87	$2.82 \times 10^{-13}$

relative abundance until a plateau was reached at approximately 40 days. Median value of the proportionality distance within the cluster was 0.42, which was compared to 1.11 between the variables selected in the cluster and all the other variables, indicating strong associations within this cluster. The OTUs were microorganisms often recovered during AD of biowaste, such as methanogenic archaea of *Methanosarcina* genus or bacteria of *Clostridiales*, *Acholeplasmatales*, and *Anaerolineales* orders. These were reported as being involved in the different steps of AD (Poirier et al., 2016). Their relative abundance increased while biowaste was degraded, until there was no more biowaste available in the bioreactor.

From the proportionality distances, we found that their abundance across time was, in proportion, similar, indicating a synchronized role during this biological process. In particular, of all the proportionality distances between the profiles of archaea of *Methanosarcina* genus and bacteria of *Clostridiales* order, the *Syntrophomonadaceae* family was the lowest which made sense as these microorganisms have already been reported as syntrophs (Liu et al., 2011); see **Supplementary Table 4**.

Their abundance was also highly associated, in proportion, to the intensity of various metabolites produced during the AD process, such as benzoic acid that is formed during the degradation of phenolic compounds (Hoyos-Hernandez et al., 2014), or phytanic acid, known to be produced during the fermentation of plant materials in the ruminant gut (Watkins et al., 2010), as well as indole-2-carboxylic acid. Thus, the identified microorganisms were likely responsible for the production of these compounds. Cluster 2 (component 1 positive) included 10

OTUs and 4 metabolites. The median value of the proportionality distance within the cluster was also very low compared to the proportionality distance outside the cluster (0.29 and 0.97; **Table 5**). Profiles of cluster 2 were negatively correlated to cluster 1, and their relative abundance decreased with time. OTUs mainly belonged to the *Bacteroidales* order. They were present in the initial inoculum but did not survive in this experiment, as the operating conditions or the substrate were not optimal for their growth, as observed in other studies (Madigou et al., 2019). Consequently, their relative abundance progressively decreased over time. Metabolites identified in cluster 2 were present in the biowaste and were degraded during the experiment. They included fatty acids (decanoic and tetradecanoic acids) that can be found in oil, or 3-(3-hydroxyphenyl)propionic acid, arising from the digestion of aromatic amino acids or breakdown product of lignin or other plant-derived phenylpropanoids. As their profile was negatively correlated to those from cluster 1, it is likely that these metabolites were consumed by OTUs assigned to cluster 1 (Torres et al., 2003). Cluster 3 (component 2 negative) included one OTU and five metabolites. Profiles relative abundance decreased slowly with time until reaching a stable abundance after 20 days. One OTU of *Clostridiales* order appeared to have been out-competed by other OTUs or phase active only during the first days of the degradation, which corresponds to the degradation of complex biopolymers contained in biowaste (Poirier et al., 2016). Among the metabolites of this cluster, hydrocinnamic and 3,4-dihydroxyhydrocinnamic acids are commonly found in plant biomass and its residues (Boerjan et al., 2003). Their molecular structure may have contributed to their slower degradation compared to other molecules, which may explain their stable abundance in the digesters until day 30. Finally, cluster 4 (component 2 positive) included 11 OTUs and 3 metabolites with slow relative abundance increase. OTUs from this group were very varied with eight orders represented. They may have had slower growth rates than OTUs of cluster 1 or were possibly involved in the degradation of molecules from cluster 3. Their abundance may also have had a slow increase as they fed on specific molecules that are only formed during the digestion process. Metabolites included N-acetylanthranilic acid and dehydroabietic acid that were likely produced by microorganisms and accumulated during the AD process, suggesting they could not be metabolized by other microorganisms.

### Integration of Microbiome, Metabolomic and Performance Data with MultiBlock sPLS

**Figure 9** illustrates the results from the integration of the three datasets, where the performance data are considered as the response of interest. Similar to the sPLS analysis, block sPLS assigned profiles to four clusters, with an average silhouette coefficient of 0.909. The proportionality distances are summarized in **Figure 10** and in **Supplementary Table 5** and show a greater level of association between profiles within each cluster, compared to the associations with all other profiles outside the cluster (see **Supplementary Figure 8** per omic variable).

Two performance variables (methane and carbon dioxide productions) were assigned to cluster 1 (component 1 negative). This result is biologically relevant, as biogas is the final output of

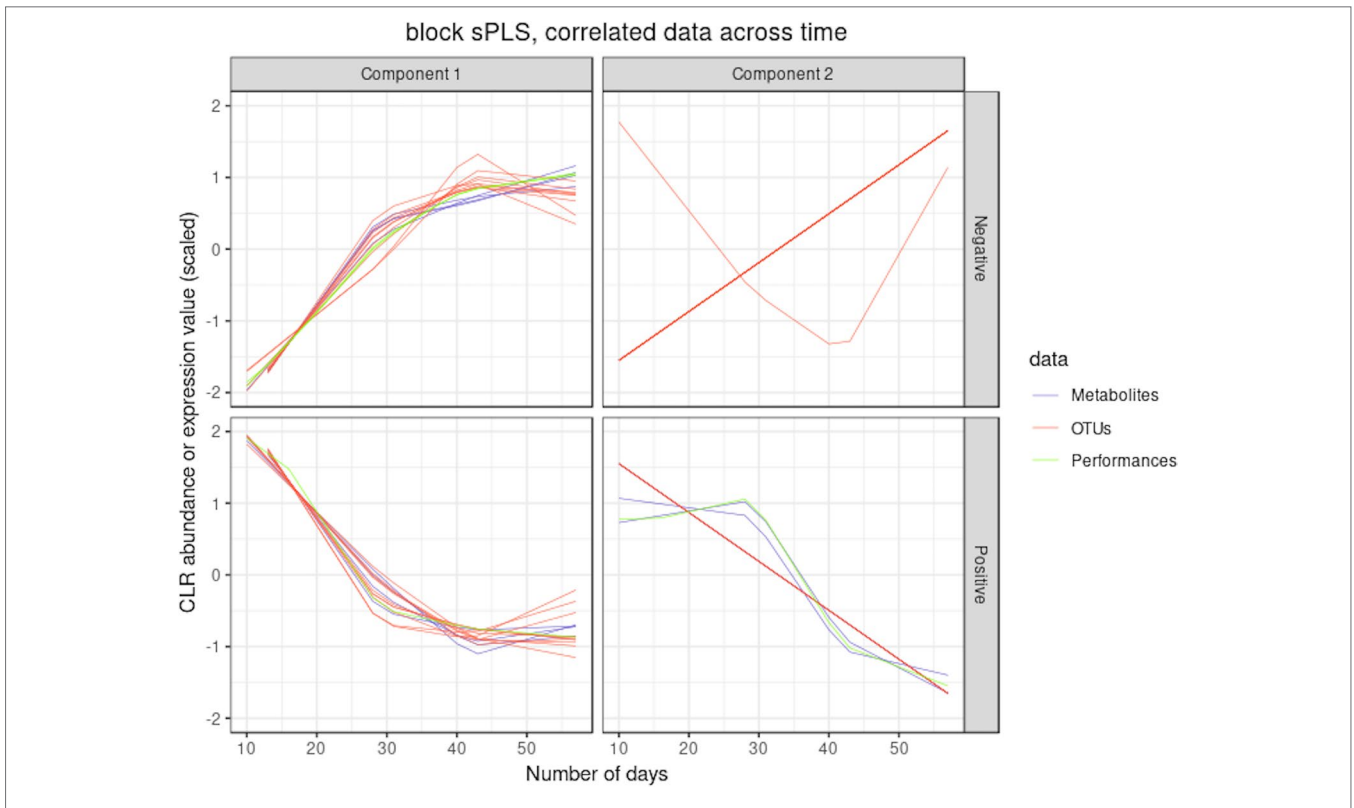


**FIGURE 9 |** Waste degradation study: integration of OTUs, metabolites and performance measures with multiblock sPLS. Each line represents the relative abundance of OTUs, metabolites and performance measures selected by multiblock sPLS across time. OTUs, metabolites and performance measures were clustered according to their contribution on each component. The clusters were further separated into profiles denoted 'positive' or 'negative' that refer to the sign of the loading vector from multiblock sPLS.

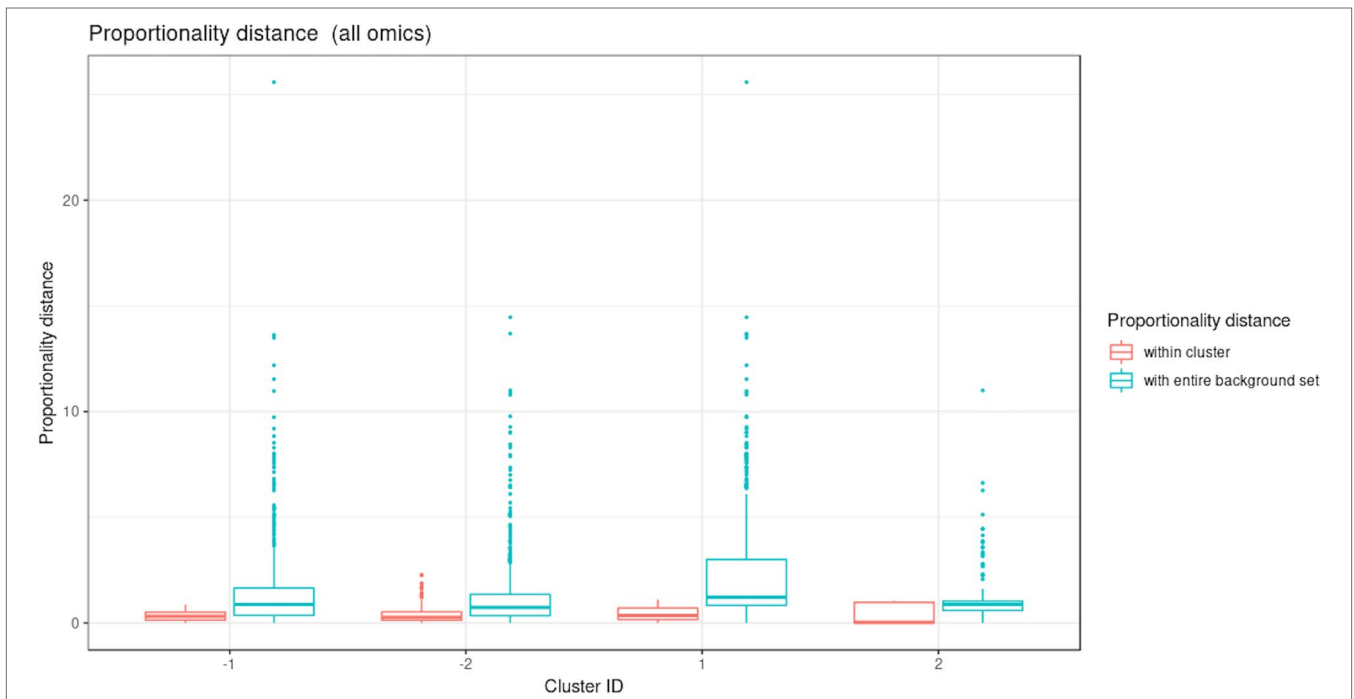


**FIGURE 10 |** Waste degradation study: Proportionality distance per cluster identified with multiblock sparse PLS. The distance was calculated between each pair of profiles within a given cluster and with the entire background set (outside a given cluster), for all omics.

the AD reaction and is known to be associated with microbial activity and growth. Moreover, it is produced by archaea, such as *Methanosarcina*, which is also selected in this cluster. The proportionality distance between this OTU and methane was very low ( $\phi_s = 0.25$ ; **Supplementary Table 4**) confirming a strong association. Cluster 1 therefore represented the progress of the degradation process. In Cluster 2 (component 1 positive), we identified acetate produced by bacteria in the early days of the incubation and consumed by archaea (cluster 1) to produce biogas. It was logically negatively associated to cluster 1 representing the progress of the degradation. Propionate was assigned to cluster 3 (component 2 positive). Its degradation was delayed compared to the molecule of cluster 1. It was expected as, for thermodynamical reasons, its degradation usually only starts when all acetate is degraded (Chapleur et al., 2014). It was biologically relevant to find it associated with hydrocinnamic and 3,4-dihydroxyhydrocinnamic acids, which are also difficult to degrade. Cluster 4 (component 2 negative) was composed of only OTUs and metabolites and was similar to the one obtained with sPLS on component 2 positive.

In summary, our framework allowed us to integrate different omic datasets measured longitudinally and identify subsets of relevant microorganisms that were highly associated with metabolites abundance and performance measures through the biodegradation process. These analyses constitute a first step toward generating novel hypotheses about the biological mechanisms underpinning the dynamics in AD.

## DISCUSSION

Advances in technology and reduced sequencing costs have resulted in the emergence of new and more complex experimental designs that combine multiple omic datasets and several sampling times from the same biological material. Thus, the challenge is to integrate longitudinal, multi-omic data to capture the complex interactions between these omic layers and obtain a holistic view of biological systems. In order to integrate longitudinal data from microbial communities with other omics, meta-omics, or other clinical variables, we proposed a data-driven analytical framework to identify highly associated temporal profiles between these multiple and heterogeneous datasets.

The application of this method allows the identification of similar expression profiles within a particular dataset (e.g., infant gut microbiota development study) but also across heterogeneous data types (16S amplicon microbiome data, metabolomics, chemical data in the waste degradation study). The clustering of longitudinal profiles helps identify groups of biological entities that may be functionally related and thus generate novel hypotheses about the regulatory mechanisms that take place within the ecosystem.

In the proposed framework, the microbial counts of the microbiota's constituent species are normalized for uneven sequencing library sizes and compositional data. Modeling with linear mixed model splines enables us to reduce the dimension of the data across the different biological replicates and take into account the individual variability due to either technical or biological sources. This approach also enables us to compare

data analyzed at different time points (e.g., the waste degradation study). Lastly, we clustered the data using multivariate dimension reduction techniques on the spline models that further allowed integration between different data types, and the identification of the main patterns of longitudinal variation.

Ribicic et al. (2018) proposed an approach similar to ours, but they applied individual PCA or sPCA on each dataset (chemical loss and microbial community) after local polynomial regression modeling. Integration was performed in a second stage of the analysis with PLS by using hierarchical clustering (Cluster Image Maps visualization) to identify correlations between the two datasets. In comparison, we offer a more complete framework that accommodates complex scenarios, across several omics and across replicates, and handles compositional data. The LMMS allows for the modeling of expression over time for each compound across biological replicates while taking into account the overall individual variability. We used sPCA, sPLS, and block sPLS as clustering means by leveraging on the loading vectors from these methods while selecting meaningful profile signatures.

Integrating different types of microbiome longitudinal data (e.g., abundance, activity, metabolic pathways, or macroscopic output) can be naively performed by concatenating all datasets. However, we showed that this approach was unsuccessful at selecting a sufficiently large number of profiles of different types and thus did not shed light on the holistic view of the ecosystem dynamics (bioreactor study). Our integrative multivariate methods sPLS and block sPLS were better suited for the integration task, as they do not merge but rather statistically correlate components built on each dataset, and thus avoid unbalance in the signature when one dataset is either more informative, less noisy, or larger than the other datasets.

When compared with fPCA, which uses either  $k$ -CFC or EM clustering algorithms, we showed that our approach led to better clustering performance. In addition, the sparse multivariate approaches sPCA and block sPLS enabled the identification of key profiles to improve biological interpretation. Note however that fPCA might be better suited than our approach for a large number of time points, as we discuss next.

We have identified several limitations in our proposed framework. First, a high individual variability between biological replicates limits the LMMS modeling step, resulting in simple linear regression models to fit the data. While a straight line model may accurately describe temporal dynamics, it could also be due to a poor quality of fit. We have implemented the Breusch–Pagan test to address this issue. Alternatively, in the case of a very high inter-individual variability that prevents appropriate smoothing, one could consider *N of One* analyses as proposed by (Gerber et al. (2012); Äijö et al. (2017) with time dynamical probabilistic models.

Second, a large number of time points can result in the modeling of noisy profiles and clusters, often due to high individual variability. Highly variable and vastly different profiles can also be difficult to cluster appropriately. Therefore, this framework is recommended when the number of time points remains small (5–10) and when regular and similar trends are expected from the data.

Third, even though our simulation results showed that the LMMS interpolation of missing time points did not seem to

impact clustering, the overall performance of the approach would be optimal for regularly spaced time points in the omics longitudinal experiments.

Fourth, we have not fully addressed the issue of analyzing time-course compositional data. Indeed, when working with relative abundances, fluctuations in the abundance of a particular microorganism might result in spurious fluctuations in the abundance of other microorganisms. This issue is not specific to microbiome data only, as other sequenced-based data are intrinsically compositional (Gloor et al., 2017). Thus, when looking for associations between longitudinal profiles, the optimal solution could be to analyze absolute abundances. However, such data require spike-ins and are currently rarely available. Badri et al. (2018) have investigated normalization strategies and their effect in correlation analysis but for a single time point, while Metwally et al. (2018) proposed three normalization strategies that ignore the compositionality data problem. No method for longitudinal compositional data analysis has been proposed as yet. The proportionality measure proposed by Lovell et al. (2015) is a promising solution to reduce spurious correlations. However, it has not been developed for longitudinal problems, and the metric is not suitable in our context to perform variable selection. Instead, we chose to use the proportionality distance as a *post hoc* evaluation in our framework, not only to reduce potential spurious associations between profiles assigned in each cluster, but also to improve and help interpretation with respect to proportional and relative abundance of the profiles.

Finally, our framework does not include time delay analysis, even though dynamic delays between different types of molecules (e.g., DNA, RNA, or metabolites) can be expected. For example, 16S data describes the abundance of the microorganisms, with metabolites as the consequence of their activity, and performance as the macroscopic resulting output. Potential delays between these molecules can be detected using other techniques, such as the fast Fourier transform approach from Straube et al. (2017), and will be further investigated in our future work.

To summarize, we have proposed one of the first computational frameworks to integrate longitudinal microbiome data with other omics data or other variables generated on the same biological samples or material. The identification of highly associated key omics features can help generate novel hypotheses to better understand the dynamics of biological and biosystem interactions. Thus, our data-driven approach

will open new avenues for the exploration and analyses of multi-omics studies.

## DATA AVAILABILITY STATEMENT

Infant gut microbiota phylochip raw data can be found in Palmer et al. (2007). The microbiome and performance datasets for the bioreactor study can be found in Poirier and Chapleur (2018); metabolomic data are available on request. In-house scripts and code to conduct both case study analysis are available in a Github public repository: <https://github.com/abodein/timeOmics>

## AUTHOR CONTRIBUTIONS

All authors contributed to the design of the study. AB and OC performed the statistical analyses. AB, OC, and K-ALC wrote the manuscript. All authors read and approved the submitted version.

## FUNDING

Waste degradation study was supported in part by the Digestomic project funded by the French National Research Agency (ANR-16-CE05-0014). K-ALC was supported in part by the National Health and Medical Research Council (NHMRC) Career Development fellowship (GNT1159458). K-ALC and OC scientific travels were supported in part by the France-Australia Science Innovation Collaboration (FASIC) Program Early Career Fellowships from the Australian Academy of Science. AB and AD are supported by Research and Innovation chair L'Oréal in Digital Biology.

## ACKNOWLEDGMENTS

We thank Angéline Guenne for analytical support with GC-MS analysis, Kodjovi Dodji Mlaga for the biological interpretations of the infant study, and Zoe Welham for proof-reading the manuscript. We thank the reviewers for their constructive comments.

## SUPPLEMENTARY MATERIAL

The Supplementary Material for this article can be found online at: <https://www.frontiersin.org/articles/10.3389/fgene.2019.00963/full#supplementary-material>

## REFERENCES

- Äijö, T., Müller, C. L., and Bonneau, R. (2017). Temporal probabilistic modeling of bacterial compositions derived from 16s rRNA sequencing. *Bioinformatics* 34, 372–380. doi: 10.1093/bioinformatics/btx549
- Aitchison, J. (1982). The statistical analysis of compositional data. *J. Royal Stat. Soc. Ser. B (Methodol.)* 44 (2), 139–160. doi: 10.1111/j.2517-6161.1982.tb01195.x
- Asnicar, F., Weingart, G., Tickle, T. L., Huttenhower, C., and Segata, N. (2015). Compact graphical representation of phylogenetic data and metadata with graphlan. *PeerJ* 3, e1029. doi: 10.7717/peerj.1029
- Badri, M., Kurtz, Z., Muller, C., and Bonneau, R. (2018). Normalization methods for microbial abundance data strongly affect correlation estimates. *bioRxiv*, 406264. doi: 10.1101/406264
- Baksi, K. D., Kuntal, B. K., and Mande, S. S. (2018). 'time': a web application for obtaining insights into microbial ecology using longitudinal microbiome data. *Front. Microbiol.* 9, 36. doi: 10.3389/fmicb.2018.00036
- Bing, M., Forney, L., and Ravel, J. (2012). The vaginal microbiome: rethinking health and diseases. *Annu. Rev. Microbiol.* 66, 371–389. doi: 10.1146/annurev-micro-092611-150157
- Boerjan, W., Ralph, J., and Baucher, M. (2003). Lignin biosynthesis. *Annu. Rev. Plant Biol.* 54, 519–546. doi: 10.1146/annurev.arplant.54.031902.134938
- Breusch, T. S., and Pagan, A. R. (1979). A simple test for heteroscedasticity and random coefficient variation. *Econ.: J. Econom. Soc.* 47 (5), 1287–1294. doi: 10.2307/1911963
- Bucci, V., Tzen, B., Li, N., Simmons, M., Tanoue, T., Bogart, E., et al. (2016). Mdsine: microbial dynamical systems inference engine for microbiome time-series analyses. *Genome Biol.* 17, 121. doi: 10.1186/s13059-016-0980-6



- Caporaso, J. G., Kuczynski, J., Stombaugh, J., Bittinger, K., Bushman, F. D., Costello, E. K., et al. (2010). Qiime allows analysis of high-throughput community sequencing data. *Nat. Methods* 7, 335. doi: 10.1038/nmeth.f.303
- Chapleur, O., Bize, A., Serain, T., Mazéas, L., and Bouchez, T. (2014). Co-inoculating ruminal content neither provides active hydrolytic microbes nor improves methanization of 13c-cellulose in batch digesters. *FEMS Microbiol. Ecol.* 87, 616–629. doi: 10.1111/1574-6941.12249
- Clemmensen, L., Hastie, T., Witten, D., and Ersbøll, B. (2011). Sparse discriminant analysis. *Technometrics* 53, 406–413. doi: 10.1198/TECH.2011.08118
- Dudek-Wicher, R. K., Junka, A., and Bartoszewicz, M. (2018). The influence of antibiotics and dietary components on gut microbiota. *Przegląd Gastroenterol.* 13, 85. doi: 10.5114/pg.2018.76005
- Durbán, M., Harezlak, J., Wand, M., and Carroll, R. (2005). Simple fitting of subject-specific curves for longitudinal data. *Stat. Med.* 24, 1153–1167. doi: 10.1002/sim.1991
- Escudé, F., Auer, L., Bernard, M., Mariadassou, M., Cauquil, L., Vidal, K., et al. (2017). Frogs: find, rapidly, otus with galaxy solution. *Bioinformatics* 34, 1287–1294. doi: 10.1093/bioinformatics/btx791
- Faust, K., Lahti, L., Gonze, D., DeVos, W. M., and Raes, J. (2015). Metagenomics meets time series analysis: unraveling microbial community dynamics. *Curr. Opin. Microbiol.* 25, 56–66. doi: 10.1016/j.mib.2015.04.004
- Fernandes, A. D., Reid, J. N., Macklaim, J. M., McMurrrough, T. A., Edgell, D. R., and Gloor, G. B. (2014). Unifying the analysis of high-throughput sequencing datasets: characterizing rna-seq, 16s rna gene sequencing and selective growth experiments by compositional data analysis. *Microbiome* 2, 15. doi: 10.1186/2049-2618-2-15
- Fukuyama, J., Rumker, L., Sankaran, K., Jeganathan, P., Dethlefsen, L., Relman, D. A., et al. (2017). Multidomain analyses of a longitudinal human microbiome intestinal cleanout perturbation experiment. *PLoS Comput. Biol.* 13, e1005706. doi: 10.1371/journal.pcbi.1005706
- Gavin, P., Mullaney, J., Loo, D., Lê Cao, K. A., Gottlieb, P., Hill, M., et al. (2018). Intestinal metaproteomics reveals host-microbiota interactions in subjects at risk for type 1 diabetes. *Diabetes Care* 41, 2178–2186. doi: 10.2337/dc18-0777
- Gerber, G. K., Onderdonk, A. B., and Bry, L. (2012). Inferring dynamic signatures of microbes in complex host ecosystems. *PLoS Comput. Biol.* 8, e1002624. doi: 10.1371/journal.pcbi.1002624
- Gloor, G. B., Macklaim, J. M., Pawlowsky-Glahn, V., and Egozcue, J. J. (2017). Microbiome datasets are compositional: and this is not optional. *Front. Microbiol.* 8, 2224. doi: 10.3389/fmicb.2017.02224
- Grice, E. A., and Segre, J. A. (2011). The skin microbiome. *Nat. Rev. Microbiol.* 9, 244. doi: 10.1038/nrmicro2537
- Guidi, L., Chaffron, S., Bittner, L., Eveillard, D., Larhlimi, A., Roux, S., et al. (2016). Plankton networks driving carbon export in the oligotrophic ocean. *Nature* 532, 465. doi: 10.1038/nature16942
- Hoyos-Hernandez, C., Hoffmann, M., Guenne, A., and Mazeas, L. (2014). Elucidation of the thermophilic phenol biodegradation pathway via benzoate during the anaerobic digestion of municipal solid waste. *Chemosphere* 97, 115–119. doi: 10.1016/j.chemosphere.2013.10.045
- Huang, D. S., and Zheng, C. H. (2006). Independent component analysis-based penalized discriminant method for tumor classification using gene expression data. *Bioinformatics* 22, 1855–1862. doi: 10.1093/bioinformatics/btl190
- Hyndman, R. J., and Ullah, M. S. (2007). Robust forecasting of mortality and fertility rates: a functional data approach. *Comput. Stat. Data Anal.* 51, 4942–4956. doi: 10.1016/j.csda.2006.07.028
- Jolliffe, I. (2011). *Principal component analysis*. Berlin Heidelberg: Springer. doi: 10.1002/0470013192.bsa501
- Knight, R., Jansson, J., Field, D., Fierer, N., Desai, N., Fuhrman, J. A., et al. (2012). Unlocking the potential of metagenomics through replicated experimental design. *Nat. Biotechnol.* 30, 513. doi: 10.1038/nbt.2235
- Kunin, V., Engelbrektsen, A., Ochman, H., and Hugenholtz, P. (2010). Wrinkles in the rare biosphere: pyrosequencing errors can lead to artificial inflation of diversity estimates. *Environ. Microbiol.* 12, 118–123. doi: 10.1111/j.1462-2920.2009.02051.x
- Lê Cao, K., Rossouw, D., Robert-Granié, C., and Besse, P. (2008). A sparse PLS for variable selection when integrating omics data. *Stat. App. Genet. Mol. Biol.* 7 (1), 1–29. doi: 10.2202/1544-6115.1390
- Lê Cao, K. A., Costello, M. E., Chua, X. Y., Brazeilles, R., and Rondeau, P. (2016a). Mixmc: Multivariate insights into microbial communities. *PLoS One* 11, e0160169. doi: 10.1371/journal.pone.0160169
- Lê Cao, K. A., Costello, M. E., Lakis, V. A., Bartolo, F., Chua, X. Y., Brazeilles, R., et al. (2016b). Mixmc: a multivariate statistical framework to gain insight into microbial communities. *PLoS One* 11, e0160169. doi: 10.1371/journal.pone.0160169
- Limam, I., Guenne, A., Driss, M. R., and Mazéas, L. (2010). Simultaneous determination of phenol, methylphenols, chlorophenols and bisphenol-a by headspace solid-phase microextraction-gas chromatography-mass spectrometry in water samples and industrial effluents. *Int. J. Environ. Anal. Chem.* 90, 230–244. doi: 10.1080/03067310903267307
- Liu, P., Qiu, Q., and Lu, Y. (2011). Syntrophomonadaceae-affiliated species as active butyrate-utilizing syntrophs in paddy field soil. *Appl. Environ. Microbiol.* 77, 3884–3887. doi: 10.1128/AEM.00190-11
- Lovell, D., Pawlowsky-Glahn, V., Egozcue, J. J., Marguerat, S., and Bähler, J. (2015). Proportionality: a valid alternative to correlation for relative data. *PLoS Comput. Biol.* 11, e1004075. doi: 10.1371/journal.pcbi.1004075
- Luo, D., Ziebell, S., and An, L. (2017). An informative approach on differential abundance analysis for time-course metagenomic sequencing data. *Bioinformatics* 33, 1286–1292. doi: 10.1093/bioinformatics/btw828
- Madigou, C., Lê Cao, K. A., Bureau, C., Mazéas, L., Déjean, S., and Chapleur, O. (2019). Ecological consequences of abrupt temperature changes in anaerobic digesters. *Chem. Eng. J.* 361, 266–277. doi: 10.1016/j.cej.2018.12.003
- Metwally, A. A., Yang, J., Ascoli, C., Dai, Y., Finn, P. W., and Perkins, D. L. (2018). Metalonda: a flexible r package for identifying time intervals of differentially abundant features in metagenomic longitudinal studies. *Microbiome* 6, 32. doi: 10.1186/s40168-018-0402-y
- Morris, A., Paulson, J. N., Talukder, H., Tipton, L., Kling, H., Cui, L., et al. (2016). Longitudinal analysis of the lung microbiota of cynomolgus macaques during long-term shiv infection. *Microbiome* 4, 38. doi: 10.1186/s40168-016-0183-0
- Palmer, C., Bik, E. M., DiGiulio, D. B., Relman, D. A., and Brown, P. O. (2007). Development of the human infant intestinal microbiota. *PLoS Biol.* 5, e177. doi: 10.1371/journal.pbio.0050177
- Paulson, J. N., Talukder, H., and Bravo, H. C. (2017). Longitudinal differential abundance analysis of microbial marker-gene surveys using smoothing splines. *BioRxiv*, 099457. doi: 10.1101/099457
- Poirier, S., and Chapleur, O. (2018). Inhibition of anaerobic digestion by phenol and ammonia: Effect on degradation performances and microbial dynamics. *Data Brief* 19, 2235–2239. doi: 10.1016/j.dib.2018.06.119
- Poirier, S., Desmond-Le Quémener, E., Madigou, C., Bouchez, T., and Chapleur, O. (2016). Anaerobic digestion of biowaste under extreme ammonia concentration: identification of key microbial phylotypes. *Bioresour. Technol.* 207, 92–101. doi: 10.1016/j.biortech.2016.01.124
- Quinn, T. P., Richardson, M. F., Lovell, D., and Crowley, T. M. (2017). propr: an r-package for identifying proportionally abundant features using compositional data analysis. *Sci. Rep.* 7, 16252. doi: 10.1038/s41598-017-16520-0
- Rand, W. M. (1971). Objective criteria for the evaluation of clustering methods. *J. Am. Stat. Assoc.* 66, 846–850. doi: 10.1080/01621459.1971.10482356
- Ribicic, D., McFarlin, K. M., Netzer, R., Brakstad, O. G., Winkler, A., Throne-Holst, M., et al. (2018). Oil type and temperature dependent biodegradation dynamics-combining chemical and microbial community data through multivariate analysis. *BMC Microbiol.* 18, 83. doi: 10.1186/s12866-018-1221-9
- Ridenhour, B. J., Brooker, S. L., Williams, J. E., Van Leuven, J. T., Miller, A. W., Dearing, M. D., et al. (2017). Modeling time-series data from microbial communities. *ISME J.* 11, 2526. doi: 10.1038/ismej.2017.107
- Rohart, F., Gautier, B., Singh, A., and Lê Cao, K. A. (2017). Mixomics: an r package for omics feature selection and multiple data integration. *PLoS Computat. Biol.* 13, doi: 10.1371/journal.pcbi.1005752
- Rousseeuw, P. J. (1987). Silhouettes: a graphical aid to the interpretation and validation of cluster analysis. *J. Comput. Appl. Math.* 20, 53–65. doi: 10.1016/0377-0427(87)90125-7
- Ruppert, D. (2002). Selecting the number of knots for penalized splines. *J. Comput. Graph. Stat.* 11, 735–757. doi: 10.1198/106186002853
- Rutayisire, E., Huang, K., Liu, Y., and Tao, F. (2016). The mode of delivery affects the diversity and colonization pattern of the gut microbiota during the first year of infants' life: a systematic review. *BMC Gastroenterol.* 16, 86. doi: 10.1186/s12876-016-0498-0
- Shields-Cutler, R. R., Al-Ghalith, G. A., Yassour, M., and Knights, D. (2018). Splinctomer enables group comparisons in longitudinal microbiome studies. *Front. Microbiol.* 9, 785. doi: 10.3389/fmicb.2018.00785

- Shin, H., Pei, Z., Martinez, K. A., Rivera-Vinas, J. I., Mendez, K., Cavallin, H., et al. (2015). The first microbial environment of infants born by c-section: the operating room microbes. *Microbiome* 3, 59. doi: 10.1186/s40168-015-0126-1
- Silverman, B. W., et al. (1996). Smoothed functional principal components analysis by choice of norm. *Ann. Stat.* 24, 1–24. doi: 10.1214/aos/1033066196
- Singh, A., Shannon, C. P., Gautier, B., Rohart, F., Vacher, M., Tebbutt, S. J., et al. (2019). Diablo: an integrative approach for identifying key molecular drivers from multi-omic assays. *Bioinformatics* 35 (17), 3055–3062. doi: 10.1093/bioinformatics/bty1054
- Smith, C. A., Want, E. J., O'Maille, G., Abagyan, R., and Siuzdak, G. (2006). Xcms: processing mass spectrometry data for metabolite profiling using nonlinear peak alignment, matching, and identification. *Anal. Chem.* 78, 779–787. doi: 10.1021/ac051437y
- Straube, J., Gorse P, A. D., Huang, B., and Lê Cao, K. A. (2015). A linear mixed model spline framework for analysing time course omics data. *PLoS One* 10 (8), e0134540. doi: 10.1371/journal.pone.0134540
- Straube, J., Huang, B. E., and Lê Cao, K. A. (2017). Dynamics to identify delays and co-expression patterns across time course experiments. *Sci. Rep.* 7, 40131. doi: 10.1038/srep40131
- Straube, J., Lê Cao, K. A., and Huang, E., (2016). *lmmS: Linear Mixed Effect Model Splines for Modelling and Analysis of Time Course Data*. R package version 1.3.3.
- Tenenhaus, A., Philippe, C., Guillemot, V., Le Cao, K. A., Grill, J., and Frouin, V. (2014). Variable selection for generalized canonical correlation analysis. *Biostatistics* 15, 569–583. doi: 10.1093/biostatistics/kxu001
- Tenenhaus, A., and Tenenhaus, M. (2011). Regularized generalized canonical correlation analysis. *Psychometrika* 76, 257–284. doi: 10.1007/s11336-011-9206-8
- Thursby, E., and Juge, N. (2017). Introduction to the human gut microbiota. *Biochem. J.* 474, 1823–1836. doi: 10.1042/BCJ20160510
- Tibshirani, R. (1996). Regression shrinkage and selection via the lasso. *J. Royal Stat. Soc. Ser. B (Methodol.)* 58 (1), 267–288. doi: 10.1111/j.2517-6161.1996.tb02080.x
- Torres, B., Porras, G., García, J. L., and Díaz, E. (2003). Regulation of the mhp cluster responsible for 3-(3-hydroxyphenyl) propionic acid degradation in *Escherichia coli*. *J. Biol. Chem.* 278 (30), 27575–27585. doi: 10.1074/jbc.M303245200
- Verbyla, A. P., Cullis, B. R., Kenward, M. G., and Welham, S. J. (1999). The analysis of designed experiments and longitudinal data by using smoothing splines. *J. Royal Stat. Soc.* 48, 269–311. doi: 10.1111/1467-9876.00154
- Wang, K., Wang, B., and Peng, L. (2009). Cvp: validation for cluster analyses. *Data Sci. J.* 8, 88–93. 0904220071–0904220071. doi: 10.2481/dsj.007-020
- Watkins, P. A., Moser, A. B., Toomer, C. B., Steinberg, S. J., Moser, H. W., Karaman, M. W., et al. (2010). Identification of differences in human and great ape phytanic acid metabolism that could influence gene expression profiles and physiological functions. *BMC Physiol.* 10, 19. doi: 10.1186/1472-6793-10-19
- Witten, D. M., Tibshirani, R., and Hastie, T. (2009). A penalized matrix decomposition, with applications to sparse principal components and canonical correlation analysis. *Biostatistics* 10, 515–534. doi: 10.1093/biostatistics/kxp008
- Wold, H. (1975). "Path models with latent variables: The NIPALS approach." *Quantitative Sociology*. (New-York, USA.: Academic Press) 307–357. doi: 10.1016/B978-0-12-103950-9.50017-4
- Yao, F., Müller, H. G., Wang, J. L., et al. (2005). Functional linear regression analysis for longitudinal data. *Ann. Stat.* 33, 2873–2903. doi: 10.1214/009053605000000660
- Zhou, L., Huang, J. Z., and Carroll, R. J. (2008). Joint modelling of paired sparse functional data using principal components. *Biometrika* 95, 601–619. doi: 10.1093/biomet/asn035.

**Conflict of Interest:** The authors declare that the research was conducted in the absence of any commercial or financial relationships that could be construed as a potential conflict of interest.

The handling editor and reviewer LA declared their involvement as co-editors in the Research Topic, and confirm the absence of any other collaboration.

Copyright © 2019 Bodein, Chapleur, Droit and Lê Cao. This is an open-access article distributed under the terms of the Creative Commons Attribution License (CC BY). The use, distribution or reproduction in other forums is permitted, provided the original author(s) and the copyright owner(s) are credited and that the original publication in this journal is cited, in accordance with accepted academic practice. No use, distribution or reproduction is permitted which does not comply with these terms.